

High SNR Analysis of RIS-Aided MIMO Broadcast Channels

Dominik Semmler, Michael Joham, and Wolfgang Utschick

School of Computation, Information and Technology, Technical University of Munich, 80333 Munich, Germany

email: {dominik.semmler,joham,utschick}@tum.de

Abstract—We analyze the influence of a reconfigurable intelligent surface (RIS) on the Gram channel eigenvalues in a high signal-to-noise ratio (SNR) scenario. This allows to connect specific channel properties with the rank improvement capabilities of the RIS. In particular, fundamental limits due to a possible line of sight (LOS) setup between the base station (BS) and the RIS are derived. Furthermore, dirty paper coding (DPC) based schemes are compared to linear precoding in such a scenario and it is shown that under certain channel conditions, the performance gap between DPC and linear precoding vanishes.

Index Terms—high SNR, eigenvalues, line of sight, waterfilling

I. INTRODUCTION

RISs have drawn a lot of attention recently as they are viewed as a key technology for future communication systems (e.g., [1]). An RIS is a surface consisting of many passive low-cost elements which make it possible to enhance the propagation environment. Under perfect channel state information (CSI), which is also assumed in this article, already large improvements in the power consumption (see [1]), the energy efficiency (see [2]), and the spectral efficiency (SE) (see [3]) could be obtained when considering an RIS in the communication system. Specifically for multiple-input multiple-output (MIMO) systems, which are considered in this article, the algorithms of [4], [5], [6], [7] are available which show a clear improvement when incorporating an RIS.

Even though the performance can be improved considerably, the phase optimization is typically not intuitive due to the highly non-convex structure of the underlying problem. Additionally, it is still not entirely clear under which specific channel conditions we can expect a large improvement of the data transmission. In [8], the rank-improvement capabilities of an RIS were demonstrated and give the impression that especially for these rank-improvement scenarios a large performance gain can be expected.

Changing the effective rank of the channel matrix is directly connected with a change of its corresponding singular values. We analyze the behavior of the squared singular values which are additionally the eigenvalues of the Gram channel matrix and are referred to as Gram channel eigenvalues (GCEs) throughout this article. For conventional communication systems, the modification of the GCEs was impossible as the channel could not be manipulated. When considering RISs, however, an additional channel component via the RIS adds

up to the direct channel. The GCEs of the resulting composite channel are, therefore, different from the ones of the direct channel and can be modified by the phase optimization of the RIS. This modification of the composite channel GCEs in comparison to the direct channel GCEs is analyzed in this article. Moreover, we discuss the limitations and the resulting consequences on the performance of the MIMO system. Considering the high SNR region allows to directly transfer the observations to the SE. One particular limitation results from the fact that the RIS and the BS are typically positioned in LOS resulting in the BS-RIS channel having a low rank. If no direct channel were present, the composite channel would only consist of the channel via the RIS and the low-rank structure directly poses limitations on the composite channel. However, we will see that, despite a direct channel being present, the eigenvalue modification remains to be severely limited in this particular case. In summary, we make the following contributions in this article:

- Analysis of the Gram channel eigenvalue modification performed by the RIS and its implications on the SE at high SNR.
- Derivation of limitations evolving from the often used LOS assumption of the channel between the BS and the RIS. A multi-RIS scenario is motivated as a possible solution to these limitations.
- We show that, under certain conditions on the channel between the BS and the RIS, all Gram channel eigenvalues become similar resulting in orthogonal user channels. Therefore, the gap between DPC based methods (see [6]) and the earlier proposed linear scheme (see [7]) vanishes for an increasing number of RIS elements.

II. SYSTEM MODEL

We consider a scenario with an N_B antenna BS serving K users each having N_M antennas. Moreover, an RIS with N_R reflecting elements is available to enhance the transmission. The downlink channel from the BS to the k -th user is therefore given by

$$\mathbf{H}_k = \mathbf{H}_{d,k} + \mathbf{H}_{r,k} \mathbf{\Theta} \mathbf{H}_s \in \mathbb{C}^{N_M \times N_B} \quad (1)$$

where $\mathbf{H}_{d,k} \in \mathbb{C}^{N_M \times N_B}$ is the direct channel from the BS to the k -th user, $\mathbf{H}_{r,k} \in \mathbb{C}^{N_M \times N_R}$ is the reflecting channel from the RIS to user k , $\mathbf{\Theta} = \text{diag}(\boldsymbol{\theta}) \in \mathbb{C}^{N_R}$ with $\boldsymbol{\theta} \in \{\mathbf{z} \in \mathbb{C}^{N_R} : |z_n| = 1, \forall n\}$ is the phase manipulation at the RIS and $\mathbf{H}_s \in \mathbb{C}^{N_R \times N_B}$ is the channel from the BS to the RIS.

The stacked channel matrix, containing the channels for all the users, is defined as

$$\mathbf{H} = [\mathbf{H}_1^H, \mathbf{H}_2^H, \dots, \mathbf{H}_K^H]^H \in \mathbb{C}^{r \times N_B} \quad (2)$$

with $r = KN_M$ where we additionally assume $N_B \geq r$. Also the subchannels $\mathbf{H}_{d,k}$ and $\mathbf{H}_{r,k}$ are stacked accordingly resulting in $\mathbf{H}_d \in \mathbb{C}^{r \times N_B}$ and $\mathbf{H}_r \in \mathbb{C}^{r \times N_R}$.

III. HIGH SNR EXPRESSIONS

As performance metric, we consider the SE which for the high SNR discussion can be written (see e.g. [9]) as

$$R_{\text{DPC/Lin}} = r \log_2 P - r \log_2 r + R_{\text{DPC/Lin,Offset}} \quad (3)$$

with

$$\begin{aligned} R_{\text{DPC,Offset}} &= -\log_2 \det((\mathbf{H}\mathbf{H}^H)^{-1}), \\ R_{\text{Lin,Offset}} &= -\sum_{k=1}^K \log_2 \det(\mathbf{E}_k^T (\mathbf{H}\mathbf{H}^H)^{-1} \mathbf{E}_k) \end{aligned} \quad (4)$$

for DPC and linear precoding, respectively. Therefore, the slope w.r.t. the logarithmic power is the same for both schemes and they are only differing in their offsets. In [9], it has already been discussed that $R_{\text{DPC,Offset}} \geq R_{\text{Lin,Offset}}$, with equality for a blockdiagonal $\mathbf{H}\mathbf{H}^H$ (orthogonal user channels). Defining the eigenvalue decomposition (EVD) $\mathbf{H}\mathbf{H}^H = \mathbf{T}\mathbf{\Lambda}\mathbf{T}^H$, the offset of DPC $R_{\text{DPC,Offset}}$ can be equivalently stated as $R_{\text{DPC,Offset}} = r \log_2 \overline{\lambda_G}$ where $\overline{\lambda_G}$ is the geometric mean of the GCEs. By applying two times the inequality between the geometric and the arithmetic mean in (a) and (b), it is possible to obtain

$$\begin{aligned} -R_{\text{Lin,Offset}} &= \sum_{k=1}^K \log_2 \det(\mathbf{E}_k^T (\mathbf{H}\mathbf{H}^H)^{-1} \mathbf{E}_k) \\ &= \sum_{k=1}^K N_M \log_2 \det(\mathbf{E}_k^T (\mathbf{H}\mathbf{H}^H)^{-1} \mathbf{E}_k)^{\frac{1}{N_M}} \\ &\stackrel{(a)}{\leq} \sum_{k=1}^K N_M \log_2 \frac{1}{N_M} \text{tr}(\mathbf{E}_k^T (\mathbf{H}\mathbf{H}^H)^{-1} \mathbf{E}_k) \\ &= N_M \log_2 \prod_{k=1}^K \frac{1}{N_M} \text{tr}(\mathbf{E}_k^T (\mathbf{H}\mathbf{H}^H)^{-1} \mathbf{E}_k) \\ &= N_M K \log_2 \sqrt[K]{\prod_{k=1}^K \frac{1}{N_M} \text{tr}(\mathbf{E}_k^T (\mathbf{H}\mathbf{H}^H)^{-1} \mathbf{E}_k)} \\ &\stackrel{(b)}{\leq} N_M K \log_2 \frac{1}{K} \sum_{k=1}^K \frac{1}{N_M} \text{tr}(\mathbf{E}_k^T (\mathbf{H}\mathbf{H}^H)^{-1} \mathbf{E}_k) \\ &= r \log_2 \frac{1}{r} \text{tr}((\mathbf{H}\mathbf{H}^H)^{-1}) \\ &= -r \log_2 \frac{r}{\text{tr}((\mathbf{H}\mathbf{H}^H)^{-1})} \\ &= -r \log_2 \overline{\lambda_H} \end{aligned} \quad (5)$$

and the offset $R_{\text{Lin,Offset}}$ can, therefore, be bounded as $r \log_2 \overline{\lambda_H} \leq R_{\text{Lin,Offset}} \leq r \log_2 \overline{\lambda_G} \leq R_{\text{DPC,Offset}}$ where $\overline{\lambda_H}$ is the harmonic mean of the eigenvalues.

Using this interpretation, we can bound the difference of DPC and linear precoding in the high SNR region with the GCEs as $R_{\text{DPC}} - R_{\text{Lin}} \leq r \log_2 \frac{\overline{\lambda_G}}{\overline{\lambda_H}}$ which follows from (5). With the help of the RIS, we are now able to manipulate the channel and its corresponding GCEs. From (5), it follows that the difference of DPC and linear precoding can be expressed as

$$R_{\text{DPC}}(\boldsymbol{\theta}_{\text{Geo}}) - R_{\text{Lin}}(\boldsymbol{\theta}_{\text{Har}}) \leq r \log_2 \frac{\overline{\lambda_G}(\boldsymbol{\theta}_{\text{Geo}})}{\overline{\lambda_H}(\boldsymbol{\theta}_{\text{Har}})} \quad (6)$$

where $\boldsymbol{\theta}_{\text{Geo}}$ are the phases that are maximizing the geometric mean and $\boldsymbol{\theta}_{\text{Har}}$ are the phases that are maximizing the harmonic mean. In addition to providing a performance bound between linear precoding and DPC, this expression allows to evaluate the similarity of the GCEs. The bound ignores the fact, that orthogonal user channels (for which the performance gap is zero) can also arise for different channel eigenvalues (e.g. when $\mathbf{H}\mathbf{H}^H$ is diagonal with different diagonal entries). Equal eigenvalues are therefore only a sufficient condition for channel orthogonality.

IV. RIS OPTIMIZATION

The maximization of the SE at high SNR for DPC reads as [cf. (4)]

$$\max_{\boldsymbol{\theta}, |\theta_n|=1 \forall n} \log_2 \det(\mathbf{H}\mathbf{H}^H). \quad (7)$$

The Gram channel matrix $\mathbf{H}\mathbf{H}^H$ can be rewritten as

$$\begin{aligned} \mathbf{H}\mathbf{H}^H &= (\mathbf{H}_d + \mathbf{H}_r \boldsymbol{\Theta} \mathbf{H}_s)(\mathbf{H}_d + \mathbf{H}_r \boldsymbol{\Theta} \mathbf{H}_s)^H \\ &= \mathbf{H}_d \mathbf{H}_d^H + \mathbf{H}_d \mathbf{H}_s^H \boldsymbol{\Theta}^H \mathbf{H}_r^H + \mathbf{H}_r \boldsymbol{\Theta} \mathbf{H}_s \mathbf{H}_d^H \\ &\quad + \mathbf{H}_r \boldsymbol{\Theta} \mathbf{H}_s \mathbf{H}_s^H \boldsymbol{\Theta}^H \mathbf{H}_r^H \\ &= \mathbf{H}_d \mathbf{H}_d^H + \sum_{l=1}^{R_s} (\mathbf{H}_d \sigma_l \mathbf{v}_l \mathbf{u}_l^H \boldsymbol{\Theta}^H \mathbf{H}_r^H \\ &\quad + \mathbf{H}_r \boldsymbol{\Theta} \sigma_l \mathbf{u}_l \mathbf{v}_l^H \mathbf{H}_d^H + \mathbf{H}_r \boldsymbol{\Theta} \sigma_l^2 \mathbf{u}_l \mathbf{u}_l^H \boldsymbol{\Theta}^H \mathbf{H}_r^H) \quad (8) \\ &= \mathbf{H}_d \mathbf{H}_d^H + \sum_{l=1}^{R_s} (\mathbf{D}_l \bar{\boldsymbol{\theta}} \bar{\boldsymbol{\theta}}^H \mathbf{D}_l^H - \mathbf{H}_d \mathbf{v}_l (\mathbf{H}_d \mathbf{v}_l)^H) \\ &= \mathbf{H}_d \left(\mathbf{I} - \sum_{l=1}^{R_s} \mathbf{v}_l \mathbf{v}_l^H \right) \mathbf{H}_d^H + \sum_{l=1}^{R_s} \mathbf{D}_l \bar{\boldsymbol{\theta}} \bar{\boldsymbol{\theta}}^H \mathbf{D}_l^H \\ &= \mathbf{C} + \mathbf{Q} \end{aligned}$$

where $\mathbf{C} = \mathbf{H}_d \mathbf{P}^{R_s} \mathbf{H}_d^H$ and $\mathbf{Q} = \sum_{l=1}^{R_s} \mathbf{D}_l \bar{\boldsymbol{\theta}} \bar{\boldsymbol{\theta}}^H \mathbf{D}_l^H$. The matrices \mathbf{C} and \mathbf{Q} are constructed with $\mathbf{D}_l = [\mathbf{H}_r \text{diag}(\mathbf{u}_l) \sigma_l, \mathbf{H}_d \mathbf{v}_l]$ and $\bar{\boldsymbol{\theta}}^H = [\boldsymbol{\theta}^H, 1]$ by using the singular value decomposition $\mathbf{H}_s = \sum_{l=1}^{R_s} \sigma_l \mathbf{u}_l \mathbf{v}_l^H$ and the orthogonal projector $\mathbf{P}^{R_s} = \mathbf{I} - \sum_{l=1}^{R_s} \mathbf{v}_l \mathbf{v}_l^H$. The optimization problem now reads as

$$\max_{\boldsymbol{\theta}, |\theta_n|=1 \forall n} \log_2 \det(\mathbf{C} + \mathbf{Q}) \quad \text{s.t.} \quad \mathbf{Q} = \sum_{l=1}^{R_s} \mathbf{D}_l \bar{\boldsymbol{\theta}} \bar{\boldsymbol{\theta}}^H \mathbf{D}_l^H. \quad (9)$$

If we could choose any positive semidefinite matrix \mathbf{Q} with $\text{rank}(\mathbf{Q}) \leq R_s$ and a limited trace, the solution would result in rank-constrained waterfilling. This was analyzed in [10] and

is equivalent to performing waterfilling over the R_s smallest eigenvalues of the matrix \mathbf{C} .

Even though we are additionally limited by the characteristics of the RIS leading further restrictions on \mathbf{Q} , we will see in the simulations that the solution shares similarities with the one of rank-constrained waterfilling. The resulting maximization under the unimodular constraints can be solved with rank relaxations similar to Semidefinite Relaxation (SDR) or with local optimal algorithms. In this article, the latter approach is chosen and we opt for high SNR adjusted versions of the element-wise algorithms given in [4], [6].

Similarly, the maximization of the harmonic mean results in $\arg \max r / \text{tr}((\mathbf{H}\mathbf{H}^H)^{-1}) = \arg \min \text{tr}((\mathbf{C} + \mathbf{Q})^{-1})$ under the same constraint as in (9). If we could choose again any positive semidefinite matrix \mathbf{Q} with $\text{rank}(\mathbf{Q}) \leq R_s$ and a limited trace, the solution would also result in rank-constrained waterfilling which can be shown by combining the results of [10] and [11, Appendix B]. Even though similarities can be observed, under the additional constraints of the RIS, the harmonic and geometric mean maximization will in general lead to different solutions.

V. EIGENVALUE BOUNDS

We will now analyze the limitations of the eigenvalue modification w.r.t. the channel conditions. To this end, we start with a rank-one assumption of the channel \mathbf{H}_s and afterwards increase the rank to an arbitrary number.

A. Rank-One Solution

Assume that the channel between the BS and the RIS is LOS dominated, e.g., when a millimeter wave (mmWave) scenario is discussed. Even though this assumption is often used, we will see that it is quite limiting in view of the resulting degrees of freedom at the RIS. For the special case $R_s = 1$, the Gram channel matrix reads as

$$\mathbf{H}\mathbf{H}^H = \mathbf{C} + \mathbf{D}_1 \bar{\boldsymbol{\theta}} \bar{\boldsymbol{\theta}}^H \mathbf{D}_1^H. \quad (10)$$

Introducing $\mathbf{W}\Phi\mathbf{W}^H = \mathbf{C}$ as the EVD (for all EVDs we assume a decreasing order of the eigenvalues) of \mathbf{C} , we know from the interlacing of eigenvalues (see for example [12, p.442, Theorem 8.5.3]), that the eigenvalues of $\mathbf{H}\mathbf{H}^H$ interlace the ones of \mathbf{C} for any possible choice of $\bar{\boldsymbol{\theta}}$.

It follows, that the GCEs of the direct channel, that is, when $\boldsymbol{\theta} = \mathbf{0}$, and the GCEs for any choice of $\boldsymbol{\theta}$ can be bounded by

$$\phi_r \leq \xi_r \leq \phi_{r-1} \leq \xi_{r-1} \leq \dots \leq \phi_1 \leq \xi_1 \quad (11)$$

where ξ_n are either the GCEs λ_n^d of $\mathbf{H}_d \mathbf{H}_d^H$ or the GCEs λ_n of $\mathbf{H}\mathbf{H}^H$. We only have equality $\phi_n = \xi_n$ if $\mathbf{e}_n^T \mathbf{W}^H \mathbf{D}_1 \bar{\boldsymbol{\theta}} = 0$ which means that the space of the rank-one update is orthogonal to $\text{range}(\mathbf{w}_n)$ where $\mathbf{w}_n = \mathbf{W}\mathbf{e}_n$ is the eigenvector corresponding to the n -th eigenvalue.

It follows immediately from (11) that the eigenvalue placement performed by the RIS is restricted by

$$\lambda_n \leq \lambda_{n-1}^d, \quad n = 2, \dots, r \quad \text{and } \lambda_1 \text{ being unbounded.} \quad (12)$$

The eigenvalues are of course further restricted by the maximum channel gain, i.e., $\lambda_n \leq \phi_n + \|\mathbf{D}_1 \bar{\boldsymbol{\theta}}\|_2^2$. We can infer from (12) that apart from the largest GCE, we can improve each GCE only up to the next larger one of the direct channel. To see this more clearly, we consider a scenario in which a group of G GCEs are very small, i.e., $\lambda_r^d \approx \lambda_{r-1}^d \approx \dots \approx \lambda_{r-G+1}^d \ll \lambda_{r-G}^d \approx \lambda_{r-G-1}^d \approx \dots \approx \lambda_1^d$ holds for the GCEs of the direct channel. In this case, the RIS could only improve one (i.e., λ_{r-G+1}^d) of the G smaller GCEs (to a maximum of approximately λ_{r-G}^d). Moreover, if the RIS has strong impact such that $\lambda_r \approx \lambda_{r-1}^d, \lambda_{r-1} \approx \lambda_{r-2}^d, \dots, \lambda_2 \approx \lambda_1^d$ holds, it can only improve the largest GCE λ_1 and the channel condition will get automatically worse. Note that when the influence of the RIS is very strong, the transmission would just take place via the rank-one RIS channel. The same could be observed, if we had a perfectly conditioned direct channel (all GCEs are approximately equal). Then the RIS could only worsen the channel condition by improving the largest GCE.

It is important to note that even if the channel \mathbf{H}_s has only a rank of one, the RIS does not deteriorate the performance. The SE will increase monotonically with a rank-one BS-RIS channel. However, the performance will be significantly degraded in comparison to a multi-rank BS-RIS channel as only a single eigenvalue can be increased without limitations.

B. Multi-Rank Solution

The eigenvalue limitations soften when the $\text{rank}(\mathbf{H}_s) = R_s$ increases. Similar to the rank-one discussion, having a total of R_s rank-one updates available, one could improve the eigenvalues up to the next R_s larger eigenvalues. Considering the rank-improvement example from above, R_s of the G eigenvalues could be improved in this scenario. Additionally, if the impact of the RIS is large, the R_s largest eigenvalues can be further improved.

We can therefore conclude that if $R_s \geq r$, all eigenvalues can be controlled and a perfectly conditioned channel (also in the extreme case, when the transmission would effectively only take place via the RIS) can be obtained.

C. Multi-RIS Scenario

Typically, strong LOS conditions for the BS-RIS channel are beneficial as can be seen by e.g. the wide-band considerations in [13]. To additionally guarantee a high rank of \mathbf{H}_s , the deployment of multiple RISs is necessary. Consequently, the maximum number of controllable eigenvalues is increased to

$$\#\text{EVs} = \sum_{n=1}^{N_{\text{RIS}}} \text{rank}(\mathbf{H}_{s,n}). \quad (13)$$

The multi-RIS scenario as a possible solution to the above eigenvalue limitations will be analyzed in a future publication.

VI. SIMULATIONS

We consider a scenario similar to the one of [3] and [7], where 6 single antenna ($N_M = 1$) users are uniformly distributed in a circle with radius 10 m centered at (200 m, 30 m) and served by an $N_B = 16$ antenna base station located

at (0 m, 0 m). The transmission is enhanced by an RIS located at (200 m, 0 m). The path losses for the channels are assumed to follow the model $L_{\text{dB}} = \alpha + \beta 10 \log_{10}(\frac{d}{\text{m}})$ (we assume $\alpha_d = \alpha_r = \alpha_s = 30$ dB for $\mathbf{H}_{d,k}$, $\mathbf{H}_{r,k}$, and \mathbf{H}_s in all simulations) where d is the distance between the receiver and the transmitter. For all plots, 1000 realizations and a noise variance of $\sigma^2 = -100$ dBm is assumed at each receive antenna. Furthermore, $\beta_d = 3.76$ and uncorrelated Rayleigh fading is assumed for $\mathbf{H}_{d,k}$ if not stated otherwise. The parameters β_r and β_s will be defined below.

A. Rank Constrained Waterfilling

At first, we will show numerically how the eigenvalues are affected by the RIS optimization. To see the impact on the eigenvalues more clearly, we introduce an extra path loss of 20 dB for 3 of the 6 users. Furthermore, the channel $\mathbf{H}_{r,k}$ is modeled as uncorrelated Rayleigh fading with $\beta_r = 3.76$. To see the importance of $\text{rank}(\mathbf{H}_s)$, we model \mathbf{H}_s with the Kronecker channel model as $\mathbf{H}_s = \sqrt{L_s} \sqrt{\frac{N_B}{R_s}} \mathbf{M} \begin{bmatrix} \mathbf{I}_{R_s} & \mathbf{0} \\ \mathbf{0} & \mathbf{0}_{N_B-R_s} \end{bmatrix} \mathbf{S}^H$ to analyze the behavior for a different rank. The elements of the matrix \mathbf{M} are distributed as $\mathcal{N}_{\mathbb{C}}(0, 1)$ and the unitary matrix \mathbf{S} is chosen by computing the QR decomposition of a random matrix where all elements are distributed as $\mathcal{N}_{\mathbb{C}}(0, 1)$. The channel gain normalization $\sqrt{\frac{N_B}{R_s}}$ is introduced as we would like to analyze the system only w.r.t. the structure (rank) of the matrix \mathbf{H}_s . The pathloss parameter for this channel is chosen as $\beta_s = 2.2$. In Figure

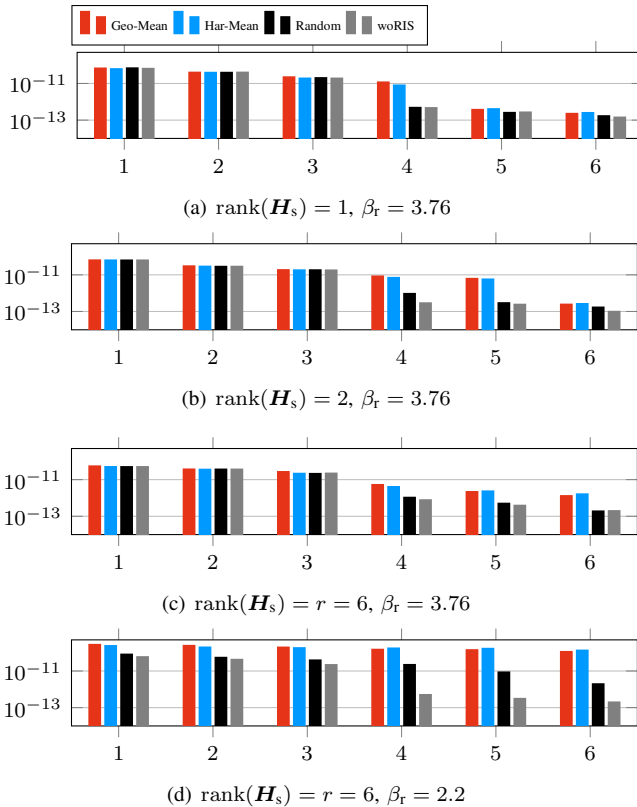


Fig. 1. GCEs for different ranks of \mathbf{H}_s and different gains of the reflective channel $\mathbf{H}_{r,k}$.

1, the eigenvalues after the RIS optimization can be seen. For the geometric mean optimization (Geo-Mean) a modified version of [6] was used. The harmonic mean maximization was performed with the algorithm presented in [7]. Both algorithms were initialized with the same random phase shifts (uniformly distributed phases) which are also presented in Figure 1 (Random).

With \mathbf{H}_s having a rank of one [see Figure 1(a)], it can be seen that the discussed limitation in (12) $\lambda_n \leq \lambda_{n-1}^d \quad \forall n = 2, \dots, 6$ holds. Therefore, only one of the 3 smaller eigenvalues could be improved.

Increasing the rank of \mathbf{H}_s to two and six results in Figure 1(b) and Figure 1(c), respectively. At first, two and then all three of the smaller eigenvalues could be improved which is in accordance with the discussion in subsection V-B. Additionally, the channel gain is spread over the controlled eigenvalues which highlights the similarities to the rank-constrained waterfilling solution mentioned in Section IV.

Furthermore, we can see in Figure 1(d) that if the RIS has enough impact ($\beta_r = 2.2$), then a rank of $\text{rank}(\mathbf{H}_s) = r = 6$ is enough to control all eigenvalues and to obtain a well-conditioned channel.

B. Performance Analysis with multi-antenna Users

We will now analyze the behavior of the eigenvalues connected with the performance of DPC and linear precoding. In comparison to the last subsection, we consider $K = 3$ users with $N_M = 2$ antennas each instead of the 6 single-antenna users. The channel $\mathbf{H}_{r,k}$ is assumed to follow uncorrelated Rayleigh fading with a channel gain of $\beta_r = 2.2$. Instead of assuming \mathbf{H}_s is rank one, we assume a more practical assumption in which \mathbf{H}_s is assumed to follow Rician fading. Particularly, a Rician component with a Rician factor of 10 dB is considered in the following. The Rician component is obtained by assuming a half-wavelength uniform linear array (ULA) at the BS and at the RIS where the angle of arrival (AoA) and angle of departure (AoD) are selected uniformly from the interval $[0, 2\pi)$. This model is then compared to \mathbf{H}_s being Rayleigh (uncorrelated) distributed.

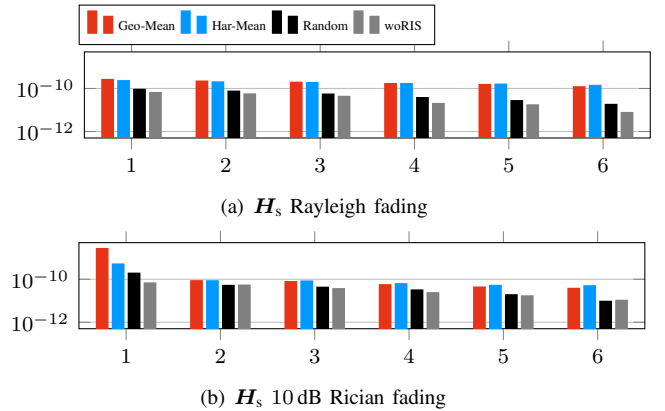


Fig. 2. GCEs for the Rayleigh and Rician fading model of the matrix \mathbf{H}_s with a power of $P = 40$ dBm and $N_R = 256$ reflecting elements.

At first, we analyze the behavior of the eigenvalues shown in

Figure 2. For Rayleigh fading [see Figure 2(a)] all eigenvalues can be controlled resulting in a well-conditioned channel. In the case of Rician fading [see Figure 2(b)], the channel has full rank as well and the smaller eigenvalues can also be improved. However, we can already see the impact of the rank-one component resulting in the increase of the largest eigenvalue. This channel characteristic directly affects the obtainable SE

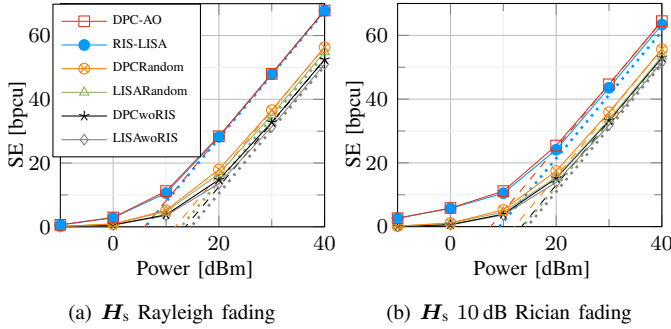


Fig. 3. Comparison of the SE with $N_R = 256$ RIS Elements for the Rayleigh and Rician fading channel model of H_s .

as seen in Figure 3 where the performance of DPC and linear precoding is compared. For DPC-AO, we use the algorithm from [6] whereas for linear precoding schemes, we use the RIS-LISA algorithm proposed in [7].

When considering only the direct channel and the random phase shifts, a performance gap can be observed between the linear schemes and DPC. In case of DPC-AO and RIS-LISA (optimized phase shifts), the performance gap only remains in the case of Rician Fading [see Figure 3(b)] whereas for Rayleigh fading [see Figure 3(a)] the methods perform similarly. This can be explained by analyzing the harmonic mean (dotted lines) and the geometric mean (dashed lines) based high SNR approximations. Please note, that for linear precoding, the lower bound in (5) instead of the exact approximation in (4) is used which allows an interpretation based on the GCEs. This means that in the high SNR region, RIS-LISA will always lie in between the mentioned lower bound and the high SNR approximation of DPC. For Rayleigh fading, the eigenvalues are similar for the optimized phase shifts and the gap between the high SNR approximations vanishes. It directly follows that RIS-LISA and DPC-AO result in a comparable performance at high SNR. Analyzing this behavior in greater depth results in Figure 4. We can see that the gap between DPC and linear precoding stays approximately constant for an increasing number of RIS elements when random phase shifts are considered. For the DPC-AO and RIS-LISA algorithms a different behavior can be observed. In the case of Rayleigh fading [see Figure 4(a)], the gap between the two schemes vanishes with an increasing number of elements whereas for Rician fading [see Figure 4(b)] the gap remains also for a higher number of elements. While the eigenvalue placement is limited (seen by the high SNR approximations), the difference between the two methods can still decrease as favorable propagation will result in orthogonal user channels for large array sizes. Furthermore, both methods perform worse in case

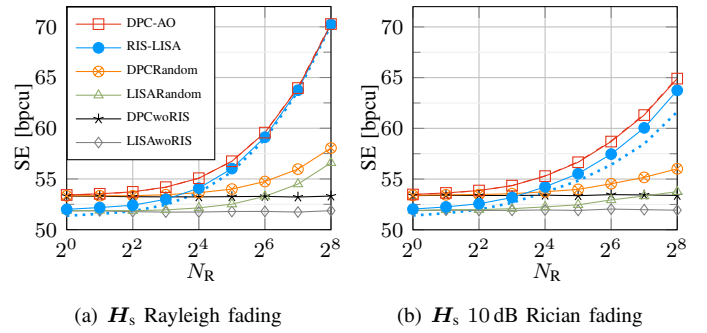


Fig. 4. Comparison of the SE with a power of $P = 40$ dBm for the Rayleigh and Rician fading channel model of H_s .

of Rician fading because of the eigenvalue limitations resulting in restrictions for spatial multiplexing. These limitations can

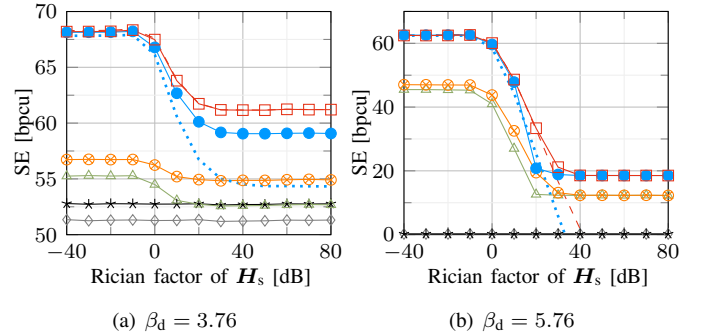


Fig. 5. Comparison of the SE with a power of $P = 40$ dBm and $N_R = 256$ reflecting elements for a different impact of the direct channel.

be further observed in Figure 5. We can see that an increasing Rician factor deteriorates the performance for both random and optimized phases due to the eigenvalue limitations. Additionally, the high-SNR approximations are not valid anymore if the Rician factor is large. This is especially pronounced for a negligible direct channel [see Figure 5(b)]. The circumstance that one eigenvalue is dominant leads to both DPC and RIS-LISA allocating only a single stream resulting in the same performance. The transmit power would have to be increased dramatically to match the high-SNR approximations.

VII. CONCLUSION

We have seen that the RIS optimization directly affects the placement of the channel eigenvalues by introducing a connection with the geometric and harmonic mean. In particular, we have seen that if the rank of the channel between the BS and the RIS is high, we can control all eigenvalues resulting in a good channel condition and the gap between linear precoding schemes and DPC vanishes. On the contrary, when the BS-RIS channel has low rank (or even only LOS), the capabilities of the RIS are clearly limited. This can be circumvented by considering multiple RISs.

REFERENCES

- [1] Q. Wu and R. Zhang, "Intelligent reflecting surface enhanced wireless network via joint active and passive beamforming," *IEEE Transactions on Wireless Communications*, vol. 18, no. 11, pp. 5394–5409, 2019.
- [2] C. Huang, A. Zappone, G. C. Alexandropoulos, M. Debbah, and C. Yuen, "Reconfigurable intelligent surfaces for energy efficiency in wireless communication," *IEEE Transactions on Wireless Communications*, vol. 18, no. 8, pp. 4157–4170, 2019.
- [3] H. Guo, Y.-C. Liang, J. Chen, and E. G. Larsson, "Weighted sum-rate maximization for reconfigurable intelligent surface aided wireless networks," *IEEE Transactions on Wireless Communications*, vol. 19, no. 5, pp. 3064–3076, 2020.
- [4] S. Zhang and R. Zhang, "On the capacity of intelligent reflecting surface aided MIMO communication," in *2020 IEEE International Symposium on Information Theory (ISIT)*, 2020, pp. 2977–2982.
- [5] C. Pan, H. Ren, K. Wang, W. Xu, M. Elkashlan, A. Nallanathan, and L. Hanzo, "Multicell MIMO communications relying on intelligent reflecting surfaces," *IEEE Transactions on Wireless Communications*, vol. 19, no. 8, pp. 5218–5233, 2020.
- [6] N. S. Perovic, L. Tran, M. Di Renzo, and M. F. Flanagan, "On the maximum achievable sum-rate of the RIS-aided MIMO broadcast channel," *arXiv*, <https://arxiv.org/abs/2110.01700>, 2021.
- [7] D. Semmler, M. Joham, and W. Utschick, "Linear precoding in the intelligent reflecting surface assisted MIMO broadcast channel," in *2022 IEEE 23rd International Workshop on Signal Processing Advances in Wireless Communication (SPAWC) (IEEE SPAWC 2022)*, Oulu, Finland, Jul. 2022.
- [8] Ö. Özdogan, E. Björnson, and E. G. Larsson, "Using intelligent reflecting surfaces for rank improvement in MIMO communications," in *ICASSP 2020 - 2020 IEEE International Conference on Acoustics, Speech and Signal Processing (ICASSP)*, 2020, pp. 9160–9164.
- [9] R. Hunger and M. Joham, "An asymptotic analysis of the MIMO broadcast channel under linear filtering," in *2009 43rd Annual Conference on Information Sciences and Systems*, 2009, pp. 494–499.
- [10] F. Gao and C. Xing, "Capacity for deterministic MIMO channels under rank constraint: A textbook derivation," in *2013 8th International Conference on Communications and Networking in China (CHINACOM)*, 2013, pp. 704–707.
- [11] M. Joham, H. Gao, and W. Utschick, "Estimation of channels in systems with intelligent reflecting surfaces," in *ICASSP 2022 - 2022 IEEE International Conference on Acoustics, Speech and Signal Processing (ICASSP)*, 2022, pp. 5368–5372.
- [12] G. H. Golub and C. F. Van Loan, *Matrix Computations*, 3rd ed. The Johns Hopkins University Press, 1996.
- [13] E. Björnson, H. Wymeersch, B. Matthiesen, P. Popovski, L. Sanguinetti, and E. de Carvalho, "Reconfigurable intelligent surfaces: A signal processing perspective with wireless applications," *IEEE Signal Processing Magazine*, vol. 39, no. 2, pp. 135–158, 2022.